Simultaneous measurement of displacement, strain and curvature in digital holographic interferometry using high-order instantaneous moments

Sai Siva Gorthi and Pramod Rastogi

Applied Computing and Mechanics Laboratory, Ecole Polytechnique Fédérale de Lausanne, 1015-Lausanne, Switzerland.

pramod.rastogi@epfl.ch

Abstract: Analysis of strain and the study of flexural moments of a deformed object is of utmost importance in non-destructive testing and evaluation. In digital holographic interferometry (DHI), this information is provided, respectively, by the first and second-order derivatives of the interference phase. This paper introduces high-order instantaneous moments based approach for the simultaneous measurement of displacement, strain and curvature distributions of a deformed object in DHI. Simulation and experimental results are presented to demonstrate the ability of the proposed method in accurately providing the direct estimation of the unwrapped distributions corresponding to the interference phase and its derivatives in a computationally efficient manner.

OCIS codes: (120.2880) Holographic interferometry; (090.1995) Digital holography; (120.4290) Nondestructive testing; (120.5050) Phase measurement.

References and links

1. F. P. Chiang and T. Y. Kao, "An optical method of generating slope and curvature contours of bent plates," Int. J. Solids Struct. **15**, 251–260 (1979).
2. Y. Y. Hung, "Shearography: A new optical method for strain measurement and nondestructive testing." Opt. Eng. **21**, 391–395 (1982).
3. D. K. Sharma, R. S. Sirohi, and M. P. Kothiyal, "Simultaneous measurement of slope and curvature with a three-aperture speckle shearing interferometr." Appl. Opt. **23**, 1542–1546 (1984).
4. P. K. Rastogi, "Visualization and measurement of slope and curvature fields using holographic interferometry: an application to flaw detection," J. Mod. Opt. **38**, 1251–1263 (1991).
5. C. J. Tay, S. L. Toh, H. M. Shang, and Q. Y. Lin, "Direct determination of second-order derivatives in plate bending using multiple-exposure shearography," Opt. Laser Technol. **26**, 91–98 (1994).
6. S. K. Bhadra, S. K. Sarkar, R. N. Chakraborty, and A. Basuray, "Coherent moire technique for obtaining slope and curvature of stress patterns," Opt. Eng. **33**, 3359–3363 (1994).
7. G. Subramanian and A. Subramanian, "Curvature contours of flexed plates by a multiple illumination moire shearing interferometer," Strain **32**, 59–62 (1996).
8. P. K. Rastogi, "Measurement of curvature and twist of a deformed object by electronic speckle-shearing pattern interferometry," Opt. Lett. **21**, 905–907 (1996).
9. K. F. Wang, A. Kiet Tieu, and E. B. Li, "Simultaneous measurement of pure curvature and twist distribution fields by a five-aperture shearing and two-Fourier filtering technique," Appl. Opt. **39**, 2577–2583 (2000).
10. F. S. Chau and J. Zhou, "Direct measurement of curvature and twist of plates using digital shearography," Opt. Laser Eng. **39**, 431–440 (2003).
11. K. F. Wang, A. K. Tieu, and M. H. Gao, "Measurement of curvature distribution using digital speckle three-shearing aperture interferometry," Opt. Laser Technol. **39**, 926–928 (2007).

#114990 - $15.00 USD Received 29 Jul 2009; revised 10 Sep 2009; accepted 13 Sep 2009; published 18 Sep 2009

12. B. Chen and C. Basaran, "Automatic full strain field moiré interferometry measurement with nano-scale resolution," Exp. Mech. **48**, 665–673 (2008).
13. G. K. Bhat, "A Fourier transform technique to obtain phase derivatives in interferometry," Opt. Commun. **110**, 279–286 (1994).
14. Q. Kemao, S. H. Soon, and A. Asundi, "Instantaneous frequency and its application to strain extraction in moire interferometry," Appl. Opt. **42**, 6504–6513 (2003).
15. Q. Kemao, S. H. Soon, and A. Asundi, "Phase-shifting windowed Fourier ridges for determination of phase derivatives," Opt. Lett. **28**, 1657–1659 (2003).
16. C. A. Sciammarella and T. Kim, "Frequency modulation interpretation of fringes and computation of strains," Exp. Mech. **45**, 393–403 (2005).
17. A. T. Andonian and S. Danyluk, "Residual stresses of thin, short rectangular plates," J. Material Sci. **20**, 4459–4464 (1985).
18. Y. Kwon, S. Danyluk, L. Bucciarelli, and J. P. Kalejs, "Residual stress measurement in silicon sheet by shadow moiré interferometry," J. Cryst. Growth **82**, 221–227 (1987).
19. F. S. Chau, S. L. Toh, C. J. Tay, and H. M. Shang, "Some examples of nondestructive flaw detection by shearography," J. Nondestruct. Eval. **8**, 225–234 (1989).
20. B. Ovryn, "Holographic interferometry," Critical Reviews in Biomedical Engineering **16**, 269–322 (1989).
21. A. Twitto, J. Shamir, A. Bekker, and A. Notea, "Detection of internal defects using phase shifting holographic interferometry," NDT and E International **29**, 163–173 (1996).
22. T. J. Mackin, K. E. Perry, J. S. Epstein, C. Cady, and A. G. Evans, "Strain fields and damage around notches in ceramic-matrix composites," J. Am. Ceram. Soc. **79**, 65–73 (1996).
23. M. R. Miller, I. Mohammed, P. S. Ho, and X. Dai, "Study of thermal deformation in underfilled flip-chip packages using high-resolution moire interferometry," American Society of Mechanical Engineers, EEP **26**, 787–793 (1999).
24. H. Xie, S. Kishimoto, J. Li, D. Zou, F. Dai, and N. Shinya, "Deformation analysis of laser processed grain oriented silicon steel sheet using moire interferometry," Materials Science Research International **5**, 291–295 (1999).
25. J. S. Ibrahim, J. N. Petzing, and J. R. Tyrer, "Deformation analysis of aircraft wheels using a speckle shearing interferometer," Proc. Inst. Mech. Eng., Part G: J. Aerospace Engg. **218**, 287–295 (2004).
26. U. Schnars and W. P. O. Juptner, "Digital recording and reconstruction of holograms in hologram interferometry and shearography," Appl. Opt. **33**, 4373–4377 (1994).
27. Y. Zou, G. Pedrini, and H. Tiziani, "Derivatives obtained directly from displacement data," Opt. Commun. **111**, 427–432 (1994).
28. M. Y. Y. Hung, L. Lin, and H. M. Shang, "Simple method for direct determination of bending strains by use of digital holography," Appl. Opt. **40**, 4514–4518 (2001).
29. C. Liu, "Simultaneous measurement of displacement and its spatial derivatives with a digital holographic method," Opt. Eng. **42**, 3443–3446 (2003).
30. W. Chen, C. Quan, and C. J. Tay, "Measurement of curvature and twist of a deformed object using digital holography," Appl. Opt. **47**, 2874–2881 (2008).
31. C. Quan, C. J. Tay, and W. Chen, "Determination of displacement derivative in digital holographic interferometry," Opt. Commun. **282**, 809–815 (2009).
32. S. S. Gorthi and P. Rastogi, "Analysis of reconstructed interference fields in digital holographic interferometry using polynomial phase transform," Meas. Sci. Technol. **20**(075307) (2009).
33. B.Porat, "Digital processing of random signals," Prentice-Hall (1994).
34. S. Golden and B. Friedlander, "A modification of the discrete polynomial transform," IEEE Trans. Sig. Proc. **46**, 1452–1455 (1998).
35. M. P. Rimmer, C. M. King, and D. G. Fox, "Computer program for the analysis of interferometric test data," Appl. Opt. **11**, 2790–2796 (1972).
36. J. Y. Wang and D. E. Silva, "Wave-front interpretation with Zernike polynomials," Appl. Opt. **19**, 1510–1518 (1980).
37. C. J. Kim, "Polynomial fit of interferograms," Appl. Opt. **21**, 4521–4525 (1982).
38. A. Cordero-Davila, A. Cornejo-Rodriguez, and O. Cardona-Nunez, "Polynomial fitting of interferograms with Gaussian errors on fringe coordinates-I: Computer simulations," Appl. Opt. **33**, 7339–7342 (1994).
39. J. Novak and A. Miks, "Least-squares fitting of wavefront using rational function," Opt. Laser Eng. **43**, 40–51 (2005).
40. E. Aboutanios and B. Mulgrew, "Iterative frequency estimation by interpolation on Fourier coefficients," IEEE Trans. Sig. Proc. **53**, 1237–1242 (2005).
41. U. Schnars and W. P. O. Juptner, "Digital recording and numerical reconstruction of holograms," Meas. Sci. Technol. **13**, R85–R101 (2002).

#114990 - $15.00 USD Received 29 Jul 2009; revised 10 Sep 2009; accepted 13 Sep 2009; published 18 Sep 2009

1. Introduction

Determining first and second-order derivatives of the interference phase is of profound importance in non-destructive testing (NDT) with applications in reliability assessment, quality control, safety monitoring, material characterization etc. as they provide information about the slope/strain and curvature/twist pertaining to a deformed object. Last two decades have witnessed an ever increasing interest in the measurement of slopes and curvatures as evident from the development of various optical interferometric techniques [1, 2, 3, 4, 5, 6, 7, 8, 9, 10, 11, 12], processing algorithms [13, 14, 15, 16], and their widespread applications [17, 18, 19, 20, 21, 22, 23, 24, 25]. Interferometric techniques employed for this task include shearography, digital holographic interferometry (DHI), and various interferometers based on Moiré. Being able to directly provide fringe maps corresponding to the slope information can be ascribed to be among the main reason behind the prominence of shearography in NDT. In the light of some of the unique advantages associated with DHI (such as allowing digital recording of holograms and facilitating numerical reconstruction), efforts have been made during recent years [26, 27, 28, 29, 30, 31] to extend its use to the measurement of slopes and curvatures. The fact that digital holography directly provides the complex amplitude of the reconstructed object wave field, and that digital shifting and multiplying with a conjugated version of a complex amplitude equivalently differentiates its phase have been exploited in the above methods. However, as the first and second-order derivatives calculated in this manner are observed to be contaminated with severe noise (in addition to being wrapped), different filtering schemes such as those based on average filter, sine/cosine transform and short-time Fourier transform have been proposed [30, 31].

This paper proposes an elegant solution for accurate and simultaneous determination of phase and its derivatives by approaching the problem from a different perspective. The reconstructed interference field in DHI is modeled as a piecewise polynomial phase signal embedded in noise. The polynomial coefficients of the phase, in each segment of the reconstructed interference field, are determined by iterating the process of calculating the high-order instantaneous moments of the signal and estimating their frequencies. The unwrapped distributions corresponding to the phase and its derivatives are then directly calculated from the estimated polynomial phase coefficients. This approach is found to provide noise-free, unwrapped distributions in a single-go. The theory of the proposed method is presented in section 2. Section 3 presents simulation and experimental results followed by conclusions in section 4.

2. High-order instantaneous moments based approach for simultaneous estimation of interference phase and its derivatives

The reconstructed interference field in digital holographic interferometry can be represented as [32]

$$A(x,y) = b(x,y)\,\exp\left[j\Delta\phi(x,y)\right] + \eta(x,y) \tag{1}$$

where $b(x,y)$, $\Delta\phi(x,y)$ and $\eta(x,y)$ represent, the amplitude, the interference phase and the noise term, respectively. The proposed technique relies on dividing each row/column of the reconstructed interference field into different segments and subsequently modeling the data in each segment with a polynomial phase signal embedded in additive complex white Gaussian noise (ACWGN). Each row of the reconstructed interference field is thus represented as a piecewise-polynomial phase signal:

$$A_{yi} = b_{yi}\,\exp(j\Delta\phi_{yi}) + \eta_{yi} \tag{2}$$

where y, i and η represent the index of the row, the index of the segment and the ACWGN with zero-mean and σ^2 variance, respectively; y and i take values from 1 to N and 1 to N_w,

#114990 - $15.00 USD Received 29 Jul 2009; revised 10 Sep 2009; accepted 13 Sep 2009; published 18 Sep 2009

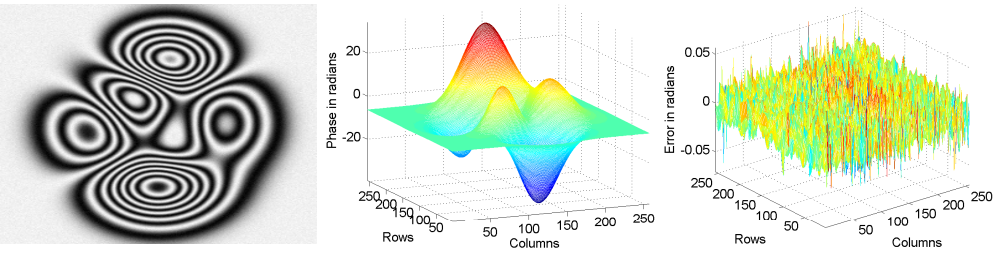

(a) (b) (c)

Fig. 1. (a) Simulated fringe pattern using the peaks function in MATLAB ($SNR = 30\,dB$, 256×256), (b) 3D mesh plot of the estimated phase distribution using the HIMs based method (c) Error in phase estimation.

respectively. If the data in each segment is approximated with a polynomial phase signal of order M, then we have:

$$g(x) = b(x)\exp\left[j\left(\sum_{q=0}^{M} a_q x^q\right)\right] + \eta(x) \tag{3}$$

The interference phase and its derivatives within each segment can then be calculated as:

$$\Delta\phi(x) = a_0 + a_1 x + a_2 x^2 + \ldots + a_M x^M \tag{4}$$

$$\frac{\partial \Delta\phi}{\partial x} = a_1 + 2a_2 x + 3a_3 x^2 + \ldots + M a_M x^{M-1} \tag{5}$$

$$\frac{\partial^2 \Delta\phi}{\partial x^2} = 2a_2 + 6a_3 x + 12a_4 x^2 + \ldots + M(M-1)a_M x^{M-2} \tag{6}$$

Equations (1)-(6) suggest that the problem of the estimation of phase and its derivatives from Eq. (1) boils down to the problem of estimating the parameters $\{a_q\}$ in Eq. (3). These coefficients can be estimated by calculating the high-order instantaneous moments (HIM) of the signal [33, 34]:

$$HIM_M[g(x), \tau_q] = \prod_{q=0}^{M-1} \left[g^{\dagger q}(x - q\,\tau_q)\right]^{\binom{M-1}{q}} \tag{7}$$

where $g^{\dagger q}(x) = \begin{cases} g(x) & \text{if } q \text{ is even} \\ g^*(x) & \text{if } q \text{ is odd} \end{cases}$

$(\cdot)^*$ denotes complex-conjugation, $\tau_1, \tau_2, .., \tau_{M-1}$ are the set of delay parameters and $\binom{x}{y} = \frac{x!}{(x-y)!\,y!}$.

Note that the HIM_M operator of the original high-order ambiguity function (HAF) method [32, 33] uses a single delay parameter τ, which is equivalent to imposing equal values to all $M-1$ delay parameters. But by considering $M-1$ different delay parameters as in Eq. (7), all of which are chosen to minimize the mean square error of the estimated coefficients [34], a considerable improvement in the accuracy of estimation can be observed, especially when the order of the polynomial approximation is three or greater. One should, moreover, note that while the original HAF method approximates the entire row with a polynomial phase signal, the present method approximates only a segment of it as such. This modification bestows several advantages as will be shown in the later part of this paper.

#114990 - $15.00 USD Received 29 Jul 2009; revised 10 Sep 2009; accepted 13 Sep 2009; published 18 Sep 2009

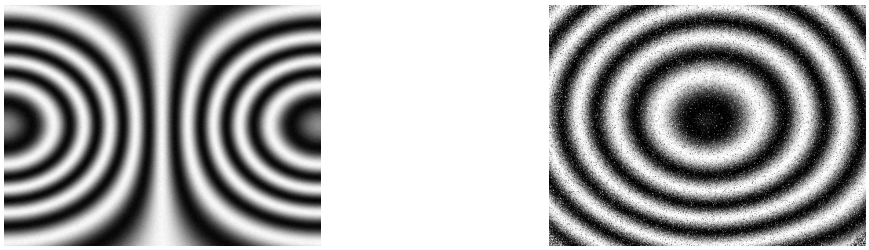

(a) (b)

Fig. 2. Patterns analyzed with the proposed method for estimating phase and their derivatives (a) Simulated fringe pattern ($SNR = 30\,dB$, 256×256) (b) Fringe pattern obtained in a DHI experiment corresponding to the central loading of a circularly clamped object (256×256).

The HIM_M operator possess an unique feature of being able to transform an M^{th} order polynomial phase signal into a single-tone whose frequency, say ω_0, is directly proportional to the highest-order polynomial coefficient a_M:

$$\hat{a}_M = \frac{\omega_0}{M!\,\gamma} \tag{8}$$

where $\gamma = \prod_{q=1}^{M-1} \tau_q$ and $\hat{a}_M$ denotes the estimate of a_M. Subsequent polynomial coefficients can be estimated by removing the effect of the highest-order phase term by 'peeling-off' the signal as $g_d(x) = g(x) \cdot \exp\left(-j\hat{a}_M x^M\right)$. The new signal $g_d(x)$ thus formed is a polynomial phase signal of the order $(M-1)$. Computing HIM_{M-1} of $g_d(x)$ results in a single-tone signal whose frequency is directly proportional to a_{M-1}. This process of estimating the highest-order coefficient in each iteration and peeling-off the signal to reduce its polynomial phase order is to be repeated until all the coefficients are estimated. After estimating all the coefficients, constructing polynomials according to Eqs.(4)-(6) results in the direct estimation of the unwrapped distributions of the interference phase and its derivatives.

Please note that the analysis of interferograms by fitting specific types of polynomials (such as Zernike polynomials) or combinations of them is an old idea and many reports have appeared [35, 36, 37, 38, 39]. But it has met with limited success as it was possible only to address specific problems since, in general, representing experimentally obtained data by polynomials is a difficult mathematical problem. Nevertheless, the approach presented in this paper overcomes this limitation by approximating the interference phase with a piecewise polynomial signal model. To illustrate the potential implication of the piecewise polynomial phase approximation, the fringe pattern shown in Fig. 1(a) is analyzed as explained in the preceding paragraphs and the estimated phase distribution is shown in Fig. 1(b). Error in phase estimation is shown in Fig. 1(c). This example confirms the ability of piecewise polynomial approximation in accurately representing even complex phase distributions (not limiting to polynomial signals) and thereby extending its applicability to wide range of applications. It is worth noting that if a typical row/column (say middle column) of the pattern shown in Fig. 1(a) is to be represented with a polynomial phase signal, polynomial of order 20 or higher is needed to achieve the accuracy shown in Fig. 1(c). Practically, it is not feasible to estimate those many coefficients by HIMs or, for that matter, by any other method. On the other hand, dividing the signal into eight segments, and approximating the data in each segment with a fourth-order polynomial signal has enabled to accurately estimate the phase. However, the choice of the number of segments and the order of polynomial approximation in each segment depends on the type

#114990 - $15.00 USD Received 29 Jul 2009; revised 10 Sep 2009; accepted 13 Sep 2009; published 18 Sep 2009

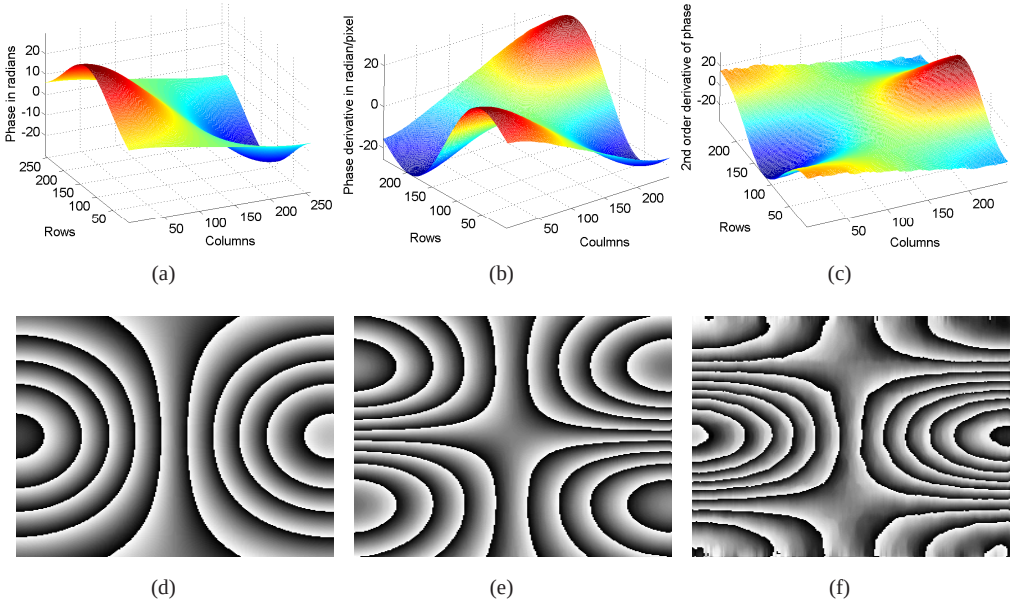

Fig. 3. 3D mesh plots of the estimated distributions from Fig. 2(a) with the proposed method corresponding to (a) interference phase, (b) first-order derivative of phase (c) second-order derivative of phase, (d), (e), (f) wrapped phase maps generated for the purpose of illustration corresponding to (a), (b) and (c) respectively.

of experiment and the functional complexity of the measured deformation. Nevertheless, dividing each row/column into eight or sixteen segments and modeling data in each segment with a fourth or second order polynomial phase signal is found to provide accurate results for many distributions, which can be considered as a general guideline. The following section presents the simultaneous determination of displacement, slope and curvature using the HIMs based approach for a typical simulated fringe pattern and for the case of central loading of a circularly clamped object in a DHI experiment.

3. Simulation and experimental results

A simulated fringe pattern (corresponding to the simulated reconstructed interference field) with a signal-to-noise ratio (*SNR*) of 30 *dB* is shown in Fig. 2(a). This pattern of dimensions 256×256 pixels (i.e. N=256) is generated using the AWGN function in MATLAB, which adds additive white Gaussian noise of a specified level to the actual signal. Applying the HIMs based estimation procedure as explained in the previous section, by segmenting each column of the signal into four pieces ($N_w = 4$) and approximating the data in each segment with a fourth-order polynomial phase signal ($M = 4$), interference phase and its first and second-order derivatives along *y*-axis are computed. We have used iterative frequency estimation by interpolation on Fourier coefficients (IFEIF) algorithm [40] for the estimation of single-tone signals' frequencies that are formed by the HIM operator. The proposed method is thus referred as HIM based rather than polynomial phase transform or HAF based [32]. We found that the use of IFEIF significantly expedites the overall estimation process of phase and its derivatives as compared to using FFT followed by an optimization routine like that of FMINBND in MATLAB. Figs. 3(a)-3(c) shows the 3-D mesh plots of the estimated continuous distributions of the interference phase and its first and second-order derivatives respectively. The corresponding wrapped dis-

#114990 - $15.00 USD Received 29 Jul 2009; revised 10 Sep 2009; accepted 13 Sep 2009; published 18 Sep 2009

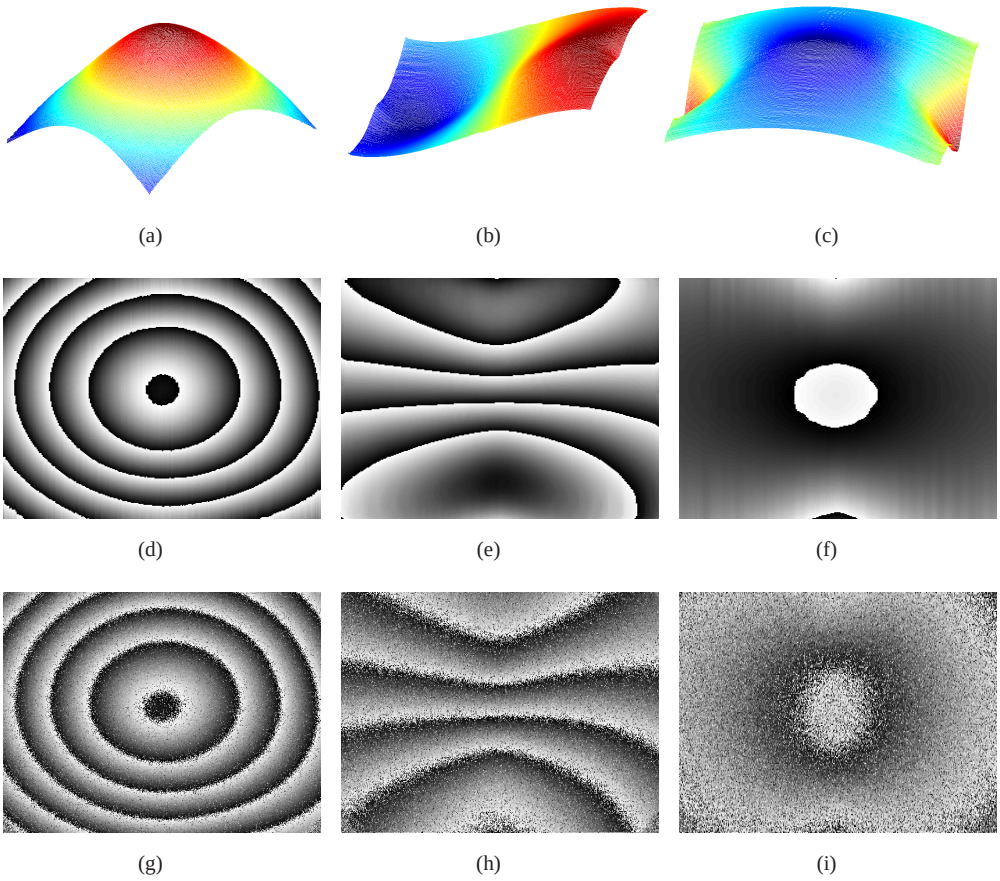

Fig. 4. 3D mesh plots of the estimated distributions from Fig. 2(b) with the proposed method corresponding to (a) out-of-plane displacement, (b) slope, (c) curvature, (d), (e), (f) wrapped maps generated for the purpose of illustration corresponding to (a), (b) and (c) respectively, (g), (h), (i) phase and its derivatives calculated using conventional direct differentiation approach shown for the purpose of comparison.

tributions, generated for the purpose of illustration are shown in Figs. 3(d)- 3(f), respectively. In order to evaluate the performance of the proposed method in terms of the accuracy of estimation, the root mean square errors (RMSE) in the estimation of phase and its derivatives by the HIMs method are calculated. Since in simulation we know the actual noise-free phase distribution, its first and second order derivatives are calculated by numerical differentiation and this information is used to calculate RMSE vales that are found to be 7.2×10^{-3}, 1.4×10^{-3} and 1.3×10^{-4} respectively.

Experimental results shown in Fig. 4 substantiate the potential utility of the proposed method for simultaneously estimating the displacement, slope and curvature in digital holographic interferometry. Two digital holograms are recorded by illuminating the test object with a Coherent Verdi laser (532 nm), one before and the other after loading the object. Discrete Fresnel transform [41] is used to perform the numerical reconstruction of the individual holograms. Since these holograms are recorded in an off-axis configuration, the real and virtual reconstructions

#114990 - $15.00 USD Received 29 Jul 2009; revised 10 Sep 2009; accepted 13 Sep 2009; published 18 Sep 2009

of the object and the undiffracted pattern can be easily separated. From the two reconstructed object wave fields obtained in this manner (one before and the other after deformation), the reconstructed interference field is formed by complex conjugate multiplication. Fig. 2(b) shows the real part of the reconstructed interference field corresponding to the central loading of a circularly clamped object (of 6 cm in diameter), located at a distance of 110 cm from the CCD camera (SONY XCL-U1000, 1628×1236). Figs. 4(a)- 4(c) show the 3-D mesh plots of the estimated continuous distributions of the displacement, slope, and curvature, respectively. The corresponding wrapped phase maps generated for the purpose of illustration are shown in Figs. 4(d)- 4(f), respectively. It can be noticed that, since the method fits polynomials with the assumption that the phase distribution that is being estimated does not contain abrupt variations such as discontinuities, the estimated phase maps are always smooth and are free from noise/spurious jumps. For the sake of comparison, direct results obtained by the conventional procedure of digital shifting and conjugate multiplication are shown in Figs. 4(g)- 4(i). As can be seen from the figures, the direct calculation method provides noisy wrapped phase maps and thereby necessitates filtering and unwrapping procedures to get continuous distributions whereas the proposed method directly provides the unwrapped estimates.

4. Conclusions

This paper has introduced a new approach for the simultaneous measurement of displacement, slope and curvature in digital holographic interferometry. The proposed approach based on high-order instantaneous moments directly provides the unwrapped distributions corresponding to the interference phase and its derivatives in a computationally efficient manner. By modeling the reconstructed interference field as a piecewise polynomial phase signal, high-order instantaneous moments based approach has made possible the simultaneous computation of phase and its derivatives. In addition to providing noise-free results, the propagation/accumulation of errors while calculating higher order derivatives from the lower-order ones is thus prevented. The method with its advantages with respect to the accuracy of estimation and computational efficiency should find great utility in non-destructive testing.

Acknowledgments

Authors would like to acknowledge the support of Swiss National Science Foundation under Grant 200020-121555.

#114990 - $15.00 USD Received 29 Jul 2009; revised 10 Sep 2009; accepted 13 Sep 2009; published 18 Sep 2009